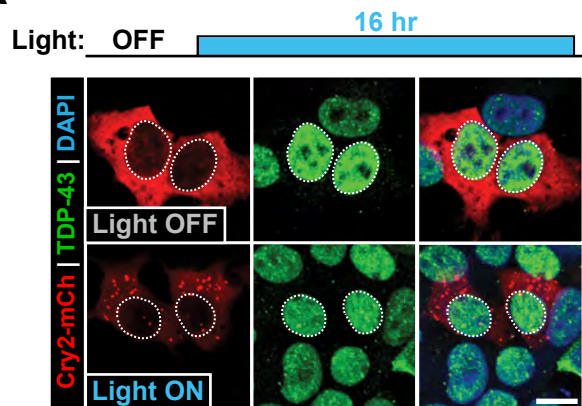


Figure S1

A



B

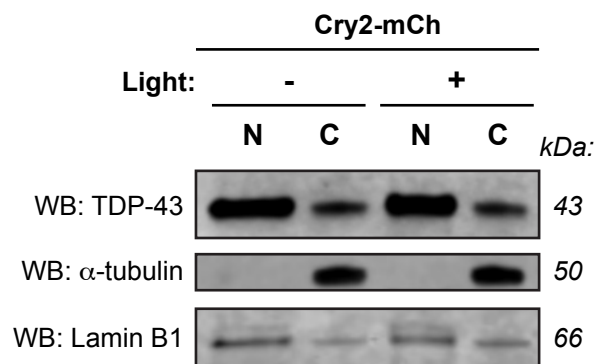
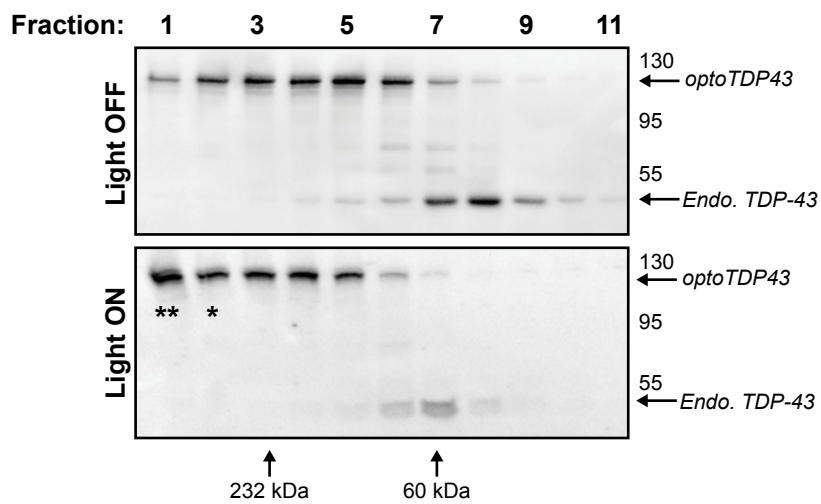


Figure S1. Chronic blue light stimulation alone does not induce mislocalization of endogenous TDP-43, Related to Figure 1.

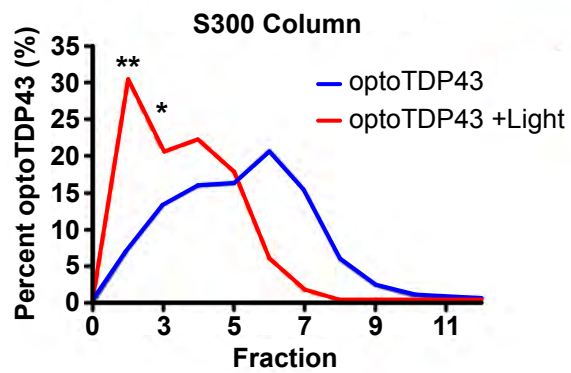
(A-B) HEK293 cells expressing Cry2olig-mCh were exposed to chronic blue light stimulation (16h, ~ 0.3 mW/cm², 465 nm) and analyzed for mislocalization of endogenous TDP-43. (A) Cells exposed to chronic blue light stimulation (bottom) or darkness (top) both show no cytoplasmic mislocalization of endogenous TDP-43 (green) by immunofluorescence. Cell nuclei are circled. (B) Cell lysates were collected following chronic blue light stimulation (lanes 3-4) or darkness (lanes 1-2) and separated into nuclear (N; lanes 1, 3) and cytoplasmic (C; lanes 2, 4) fractions. Western blot analysis of endogenous TDP-43 shows no cytoplasmic mislocalization of TDP-43 with or without blue light stimulation. Scale bar = 10 μ m.

Figure S2

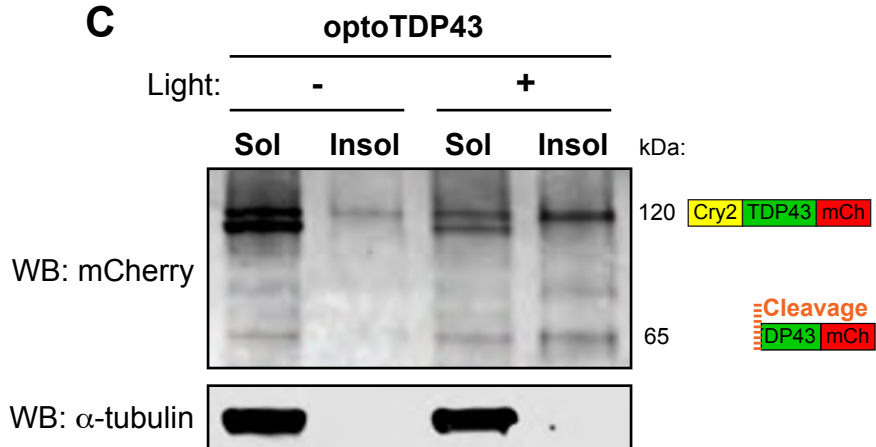
A



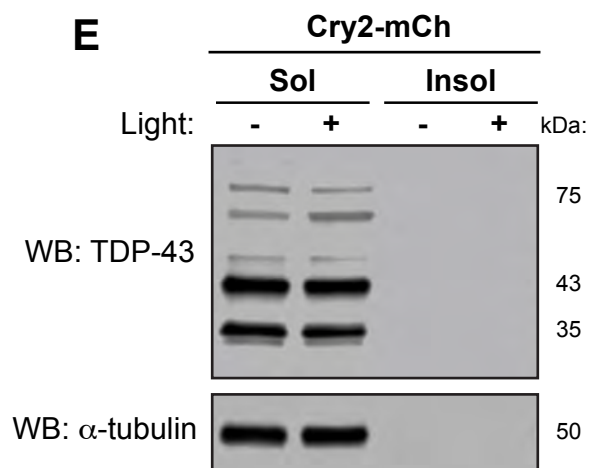
B



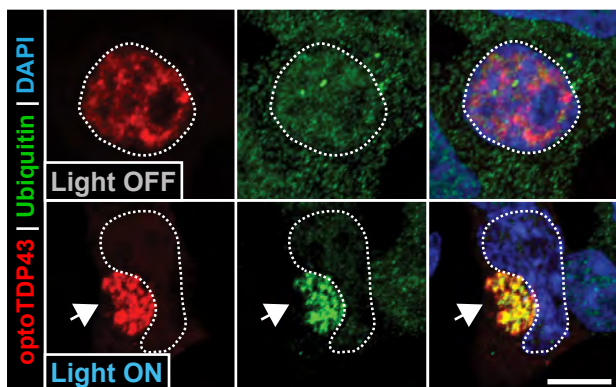
C



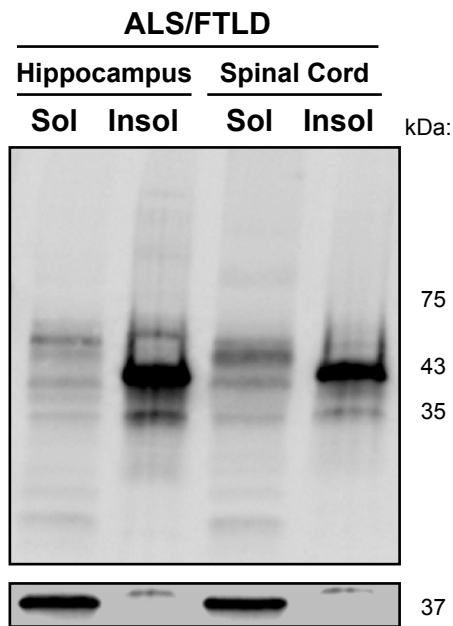
E



G



D



F

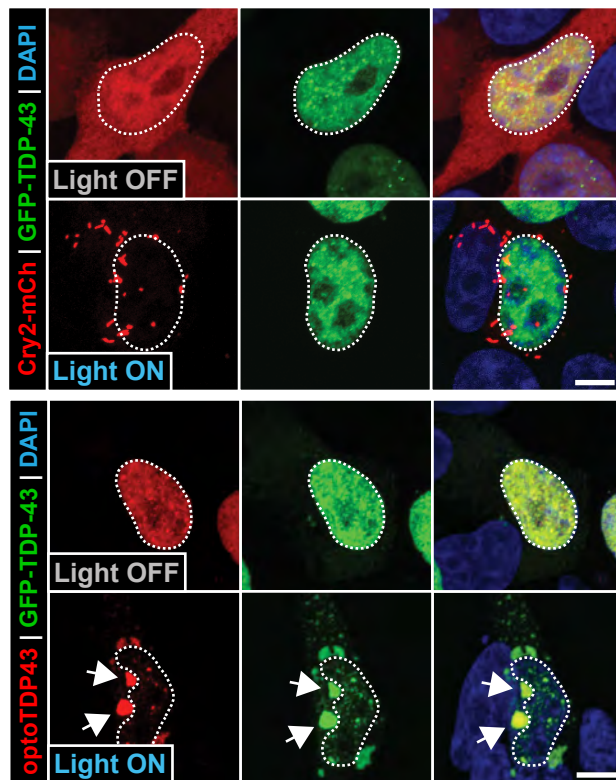


Figure S2. Chronic blue light stimulation promotes the formation of high-molecular-weight optoTDP43 oligomers and recruitment of non-optogenetic TDP-43 to inclusions, Related to Figure 1.

(A-B) Cell lysates from HEK293 cells expressing optoTDP43 were collected and analyzed by size exclusion chromatography. Samples were collected from cells either exposed to stimulation with blue light (16h, $\sim 0.3\text{mW/cm}^2$, 465 nm, bottom) or kept in darkness (top). The void volume of the column was determined with blue dextran (2000 kDa). Column fractions were subjected to SDS-PAGE and western blot analysis for TDP-43. The molecular weight standards are indicated to the right of the representative blots. The elution peak of column size standards (232 kDa and 60 kDa) are indicated by arrows at the bottom of the gel. (B) optoTDP43 proteins exposed to blue light stimulation demonstrate a shift towards higher-molecular weight species (fractions 1-3, indicated by asterisks), indicating light-induced oligomerization. (C) Lysates from optoTDP43-expressing cells exposed to chronic blue light treatment (16h, $\sim 0.3\text{mW/cm}^2$, 465 nm) or darkness were collected and separated into detergent-soluble (lanes 1, 3) and RIPA-insoluble, urea-soluble (lanes 2, 4) fractions. Western blot analysis of mCherry proteins shows an enhanced shift of full-length and n-terminal cleaved optoTDP43 products in the detergent-insoluble fraction. (D) ALS/FTLD patient tissue from the hippocampus and spinal cord was separated into detergent-soluble (lanes 1, 3) and RIPA-insoluble, urea-soluble (lanes 2, 4) fractions prior to western blot analysis of TDP-43. (E) Cell lysates collected from Cry2-mCh-expressing cells following chronic blue light stimulation (lanes 2, 4) or darkness (lanes 1, 3) were separated into detergent-soluble (lanes 1, 2) and RIPA-insoluble, urea-soluble (lanes 3, 4) fractions. Western blot analysis probing for endogenous TDP-43 shows no recruitment of TDP-43 to the insoluble fraction with or without chronic blue light stimulation. (F) To confirm the ability of optoTDP43 to recruit non-optogenetic TDP-43 species into light-induced inclusions, HEK293 cells were co-transfected with either optoTDP43 (bottom) or the photoreceptor-only control Cry2olig-mCh (top) and EGFP-TDP43. optoTDP43-expressing cells exposed to chronic blue light stimulation (16h, $\sim 0.3\text{mW/cm}^2$, 465 nm) show co-localization of light-induced inclusions with EGFP-TDP43 (indicated by arrows). Light-induced Cry2olig-mCh clusters show no co-localization with EGFP-TDP43 signal, indicating a TDP-43:TDP-43 interaction-dependence of recruitment to induced optoTDP43 inclusions. Cell nuclei are circled. Scale bar = 10 μm . (G) Cells expressing optoTDP43 were exposed to chronic blue light stimulation (16h, $\sim 0.3\text{mW/cm}^2$, 465 nm, bottom) or darkness (top) and immunostained for ubiquitin (green). Light-induced optoTDP43 inclusions strongly co-localize with ubiquitin signal (indicated by arrows). Cell nuclei are circled. Scale bar = 10 μm .

Figure S3

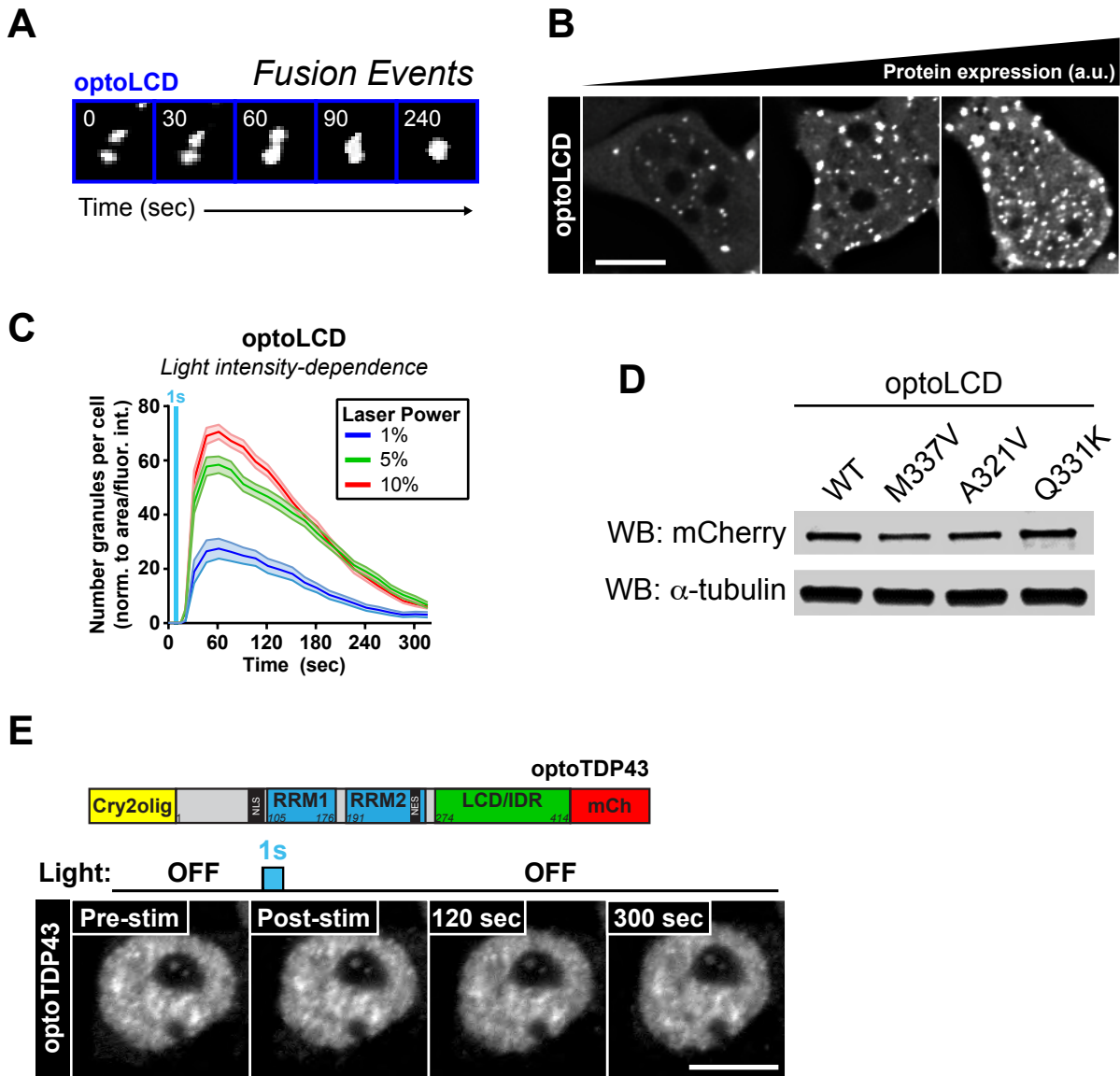


Figure S3. optoLCD granules display properties of phase-separated droplets and full-length optoTDP43 does not form optoDroplets, Related to Figure 2.

(A) Representative images of individual optoLCD granules showing fusion events following acute blue light stimulation (1 sec, 1% laser power, 488 nm). optoLCD granules underwent fusion and subsequent relaxation upon granule:granule contact, suggesting a liquid-like state of light-induced LCD granules. (B) Representative images of optoLCD particle formation following acute blue light stimulation (1 sec, 1% laser power, 488 nm) in cells expressing increasing concentrations of optoLCD proteins (as determined by relative fluorescence intensity). (C) Cells expressing optoLCD were exposed to acute blue light stimulation of increasing laser intensity (1 sec, 1-10% as indicated, 488 nm) and normalized granule number per cell was tracked over time. optoLCD proteins displayed enhanced phase transition responses following acute blue light stimulation of increasing light input, indicating a tunable property of light-induced LCD phase transitions as a function of activated photoreceptor molecules. $n = 25-67$ cells per laser setting. (D) Western blot analysis of WT and mutant optoLCD protein expression levels. (E) Full-length optoTDP43 was expressed in HEK293 cells exposed to acute blue light stimulation (1 sec, 10% laser power, 488 nm) to determine whether full-length TDP-43 could undergo LIPS. No optoTDP43 granule formation was observed in response to acute blue light stimulation. Data shown are mean \pm S.E.M. Scale bars = 10 μ m.

Figure S4

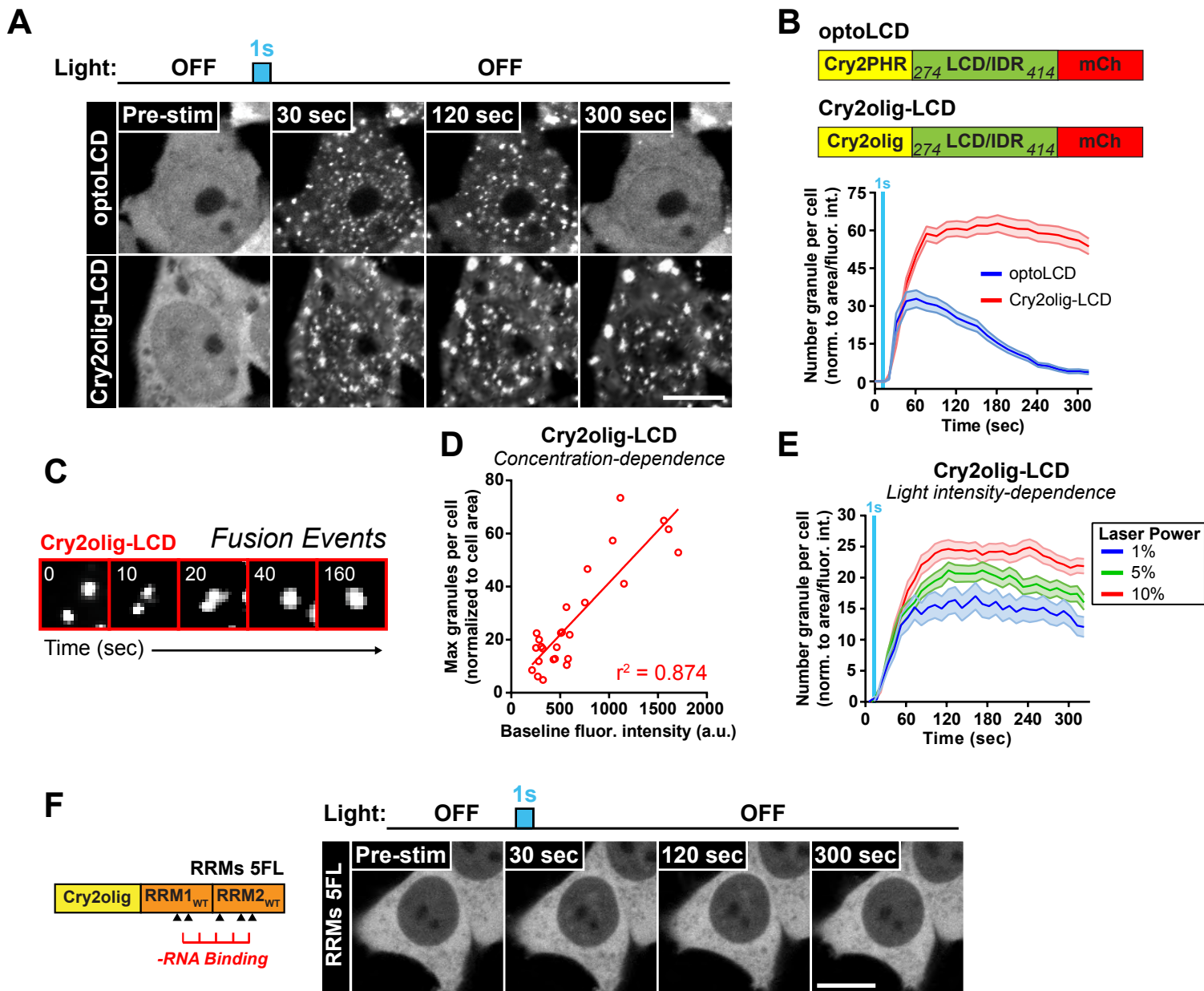


Figure S4. Cry2olig-LCD confers an enhanced phase separation response to light, Related to Figure 3.

(A-B) HEK293 cells expressing either optoLCD (top) or the Cry2olig modified photoreceptive domain fused to the TDP-43 LCD (Cry2olig-LCD, bottom) were subjected to acute blue light stimulation (1 sec, 1% laser power, 488 nm) and granule formation was tracked over time. (B) Quantification of normalized granules per cell over time shows an enhanced phase transition response to light when the TDP-43 LCD is fused to the Cry2olig domain versus the WT Cry2PHR domain. $n = 25-48$ cells per construct. Data shown are mean \pm S.E.M. (C) Representative images of individual Cry2olig-LCD granules undergoing fusion events following acute blue light stimulation (1 sec, 1% laser power, 488 nm). As was observed with optoLCD droplets, Cry2olig-LCD granules underwent fusion and relaxation upon granule:granule contact. (D) A Pearson's correlation was executed to analyze the protein concentration-dependence of Cry2olig-LCD phase transitions in response to acute blue light stimulation (1 sec, 10% laser power, 488 nm). Baseline fluorescence intensity was plotted against maximum granule number per cell during the imaging period. Data points shown are representative of individual cells. $n = 26$ cells. (E) Cry2olig-LCD-expressing cells were exposed to acute blue light stimulation of increasing laser intensity (1 sec, 1-10% as indicated, 488 nm) and normalized granule number per cell was quantified post-stimulation. Again, an enhanced phase separation response was observed following blue light stimulation of increasing intensity. $n = 50-81$ cells per laser setting. (F) Cells expressing a protein containing the TDP-43 RRM with RNA-binding mutations fused to the Cry2olig photoreceptor (RRMs 5FL) were exposed to acute blue light stimulation (1 sec, 10% laser power, 488nm). No droplet formation is observed following light stimulation, suggesting the TDP-43 LCD is necessary for LIPS behavior. Data shown are mean \pm S.E.M. Scale bars = 10 μ m.

Figure S5

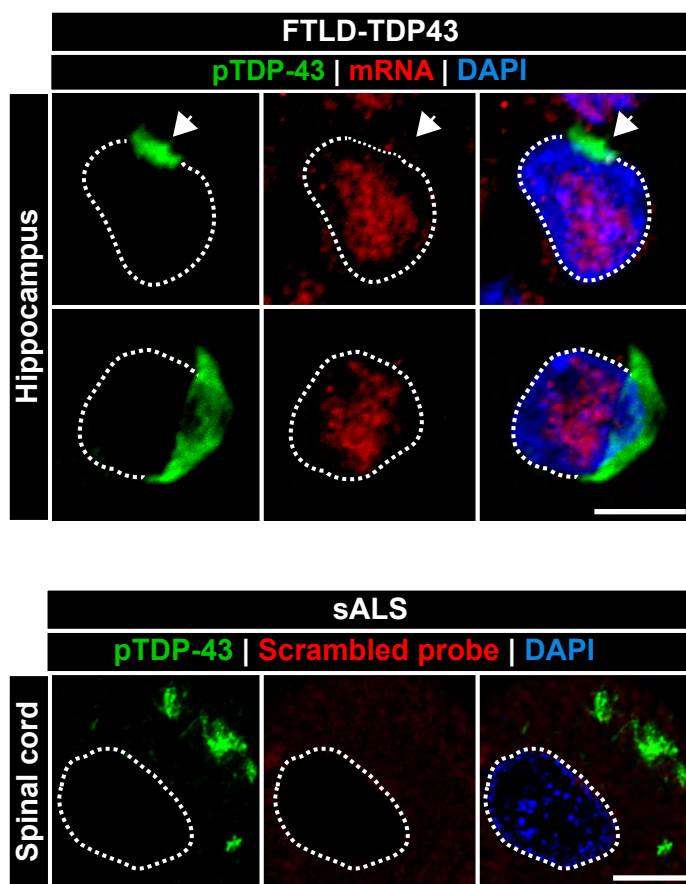
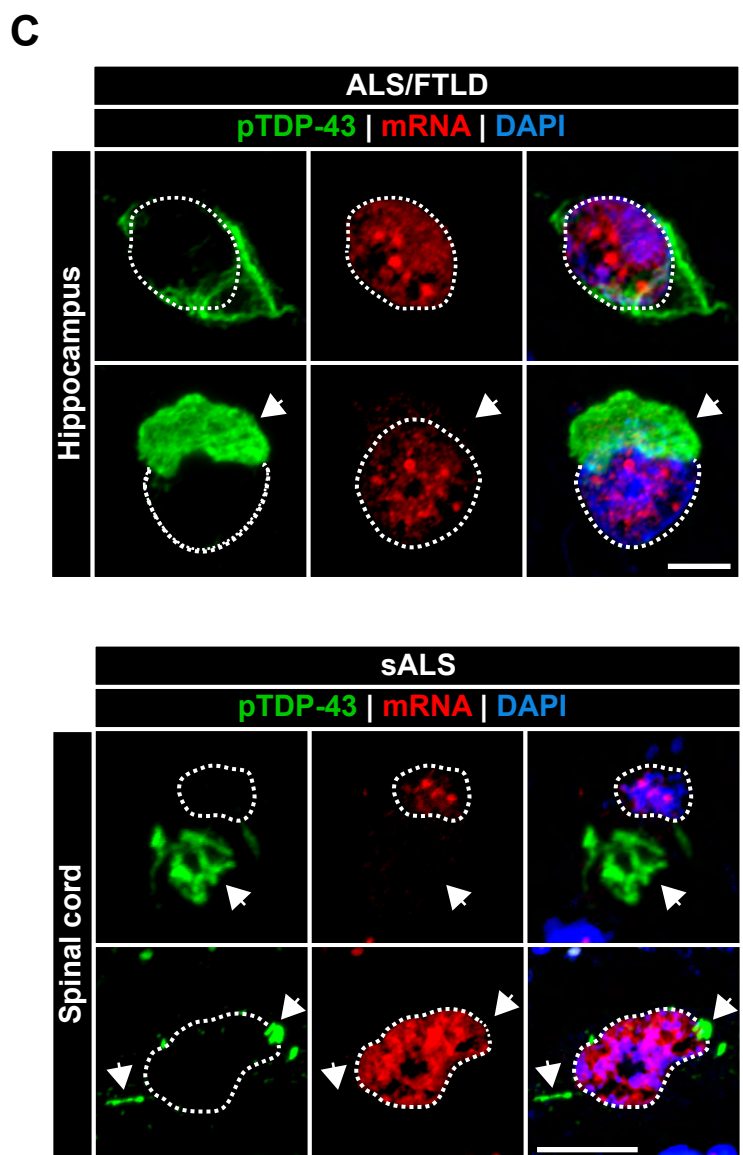
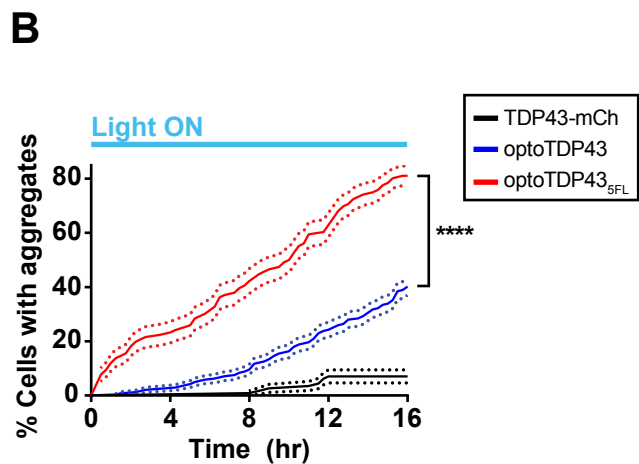
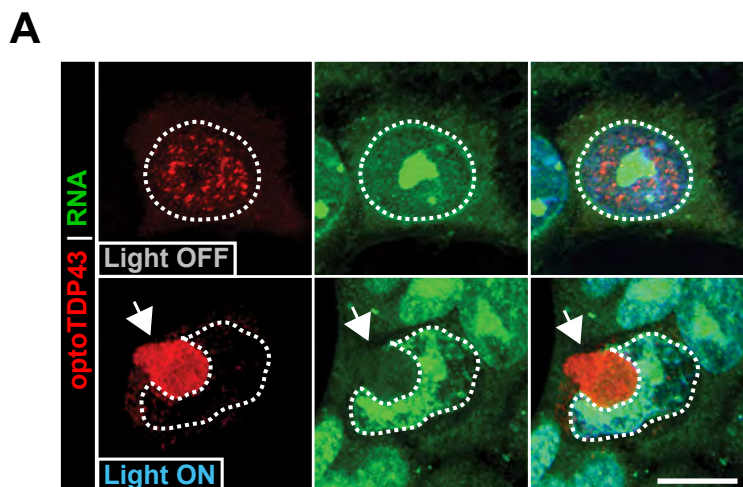


Figure S5. TDP-43 inclusions in patient tissue and optoTDP43 system show an absence of RNA, Related to Figure 3.

(A) optoTDP43 was expressed in HEK293 cells that were exposed to chronic blue light stimulation (16h, $\sim 0.3\text{mW}/\text{cm}^2$, 465 nm) to induce optoTDP43 inclusion formation. Cells were then fixed in ice-cold methanol and stained with SYTO RNaselect non-selective RNA dye to determine whether optoTDP43 inclusions contained any RNA species, in addition to mRNA. optoTDP43 inclusions do not appear to co-stain with SYTO RNaselect dye, suggesting there are no RNA species contained within inclusions. (B) HEK293 cells expressing WT optoTDP43 (blue), RNA-binding-deficient optoTDP43 5FL (red), or non-optogenetic TDP43-mCh (black) were chronically stimulated with blue light ($\sim 0.3\text{mW}/\text{cm}^2$, 465 nm) and simultaneously imaged over time in an automated microscopy screen to assess whether RNA-binding affects full-length TDP-43 inclusion formation. Quantification of percentage of cells with inclusions over time shows a significantly increased rate of light-induced inclusion formation with reduced RNA-binding efficiency (optoTDP43 5FL, red). $n = 113\text{-}239$ cells per construct. (C) Additional representative images of mRNA FISH analysis of ALS/FTLD patient tissue. Hippocampal and spinal cord sections from two FTLD cases (*C9ORF72*-FTLD, top left; FTLD-TDP43, top right) and one ALS case (sporadic ALS, bottom left) were examined by immunohistochemistry and RNA FISH. In all cases, no co-localization was observed between mRNA and pTDP-43 signal. Data shown are mean \pm S.E.M. ****, $p < .0001$. Cell nuclei are circled. Scale bars = 10 μm .

Figure S6

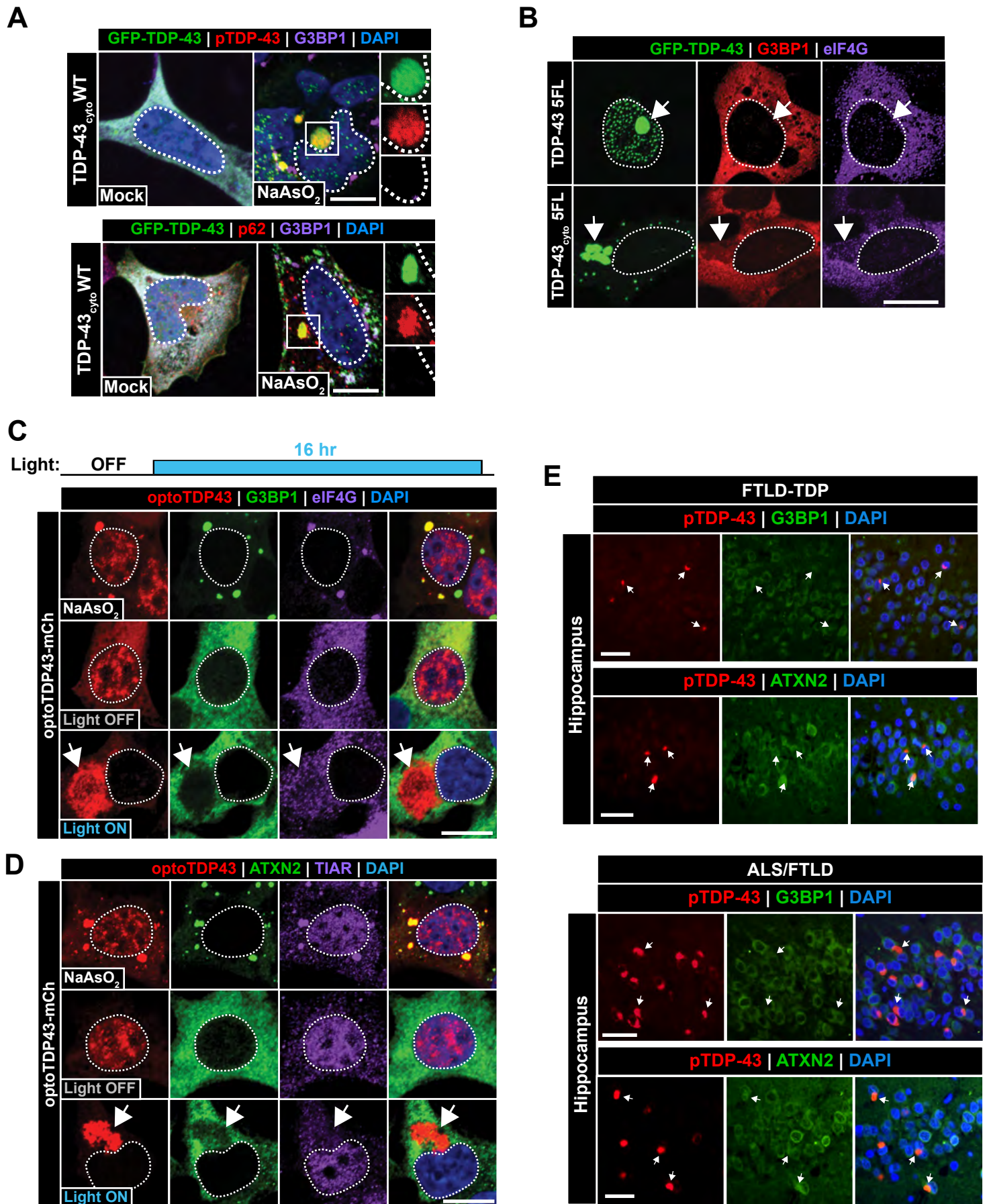


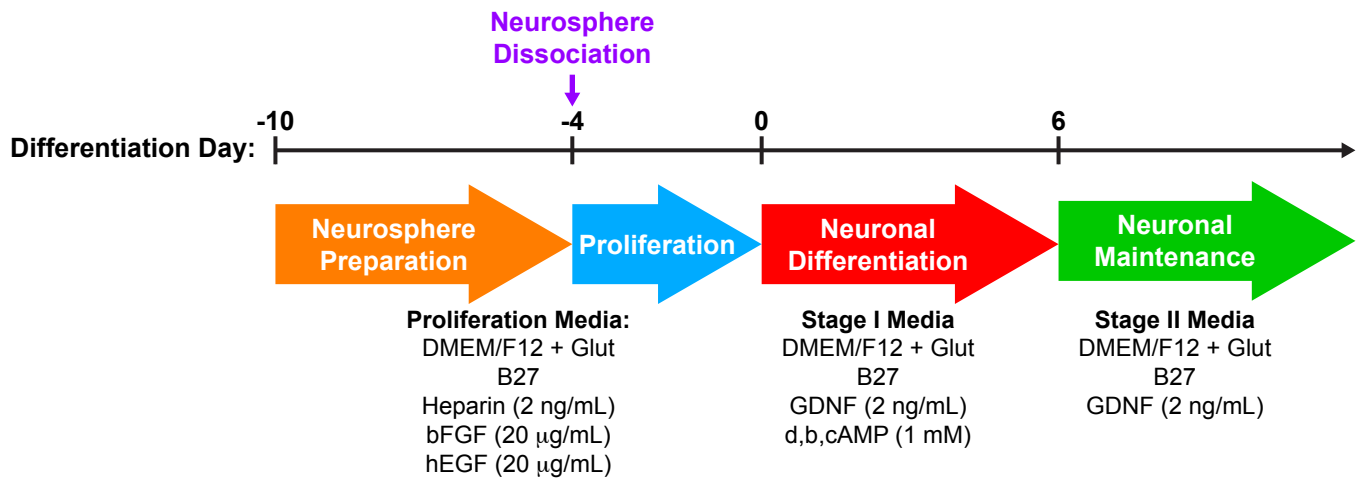
Figure S6. RNA-deficient TDP-43 inclusions do not co-localize with stress granule components, Related to Figure 5.

(A) HEK293 cells expressing EGFP-TDP43_{cyto} were immunostained for hyperphosphorylated TDP-43 (top row, red) or p62 (bottom row, red) and G3BP1 (purple) following sodium arsenite treatment. (B) Representative images of cells containing TDP-43 5FL and TDP-43_{cyto} 5FL inclusions immunostained for stress granule proteins G3BP1 (red) and eIF4G (purple).

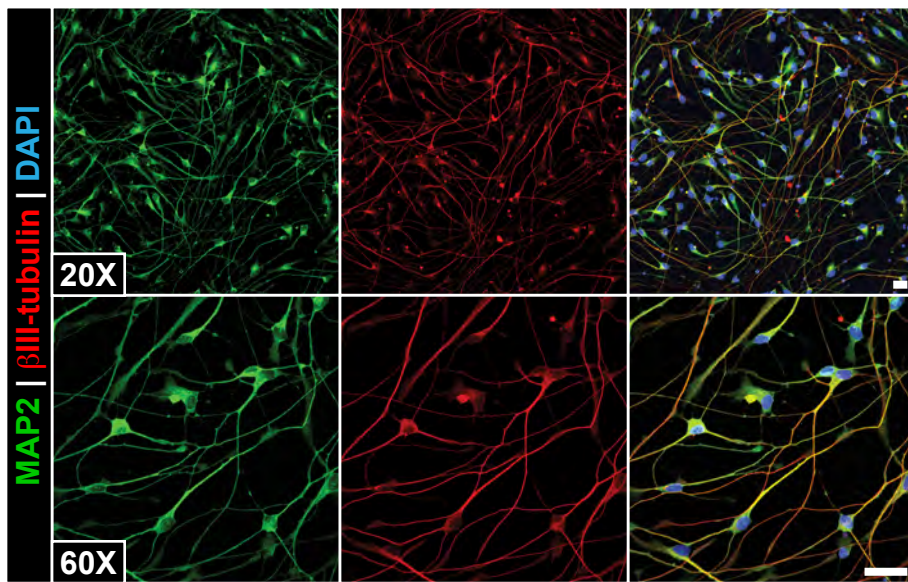
(C-D) HEK293 cells expressing optoTDP43 were subjected to sodium arsenite treatment (top row), chronic blue light stimulation (16 hr, ~0.3 mW/cm², 465 nm) (bottom row), or darkness (middle row) and immunostained for known stress granule components G3BP1 (green) and eIF4G (purple) (C) or ATXN2 (green) and TIAR (purple) (D). Cells treated with sodium arsenite (top row) show that optoTDP43 can be recruited to stress granules through the activation of endogenous cellular stress pathways. However, optoTDP43 inclusions (indicated by arrows) induced with blue light stimulation do not co-localize with any of the tested stress granule markers. Scale bars = 10 μm. Cell nuclei are circled. (E) Representative images of neuropathological examination of TDP-43 inclusions and SG component proteins (G3BP1, top rows; ATXN2, bottom rows) in FTLN-TDP and ALS/FTLN hippocampal sections. Arrows indicate lack of co-localization between SG components and TDP-43 inclusions. Scale bars = 50 μm.

Figure S7

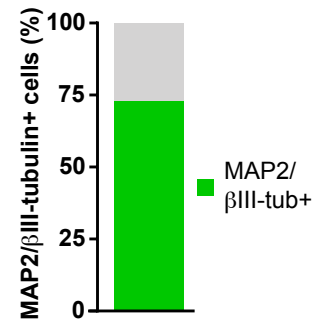
A



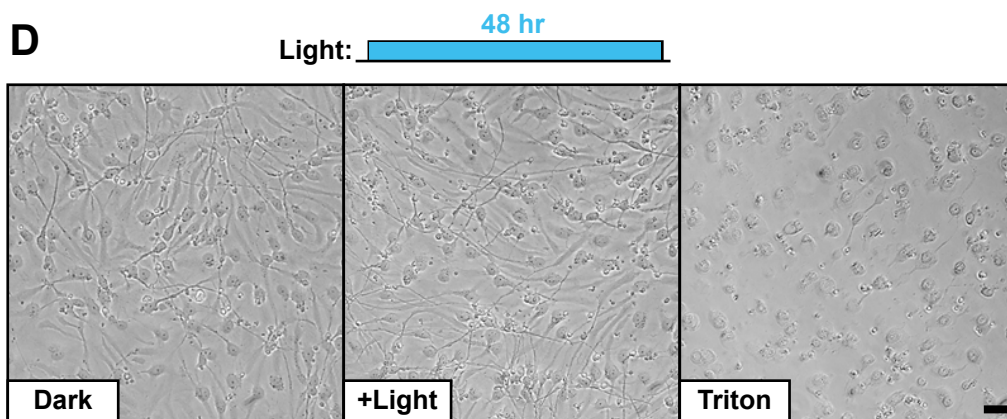
B



C



D



E

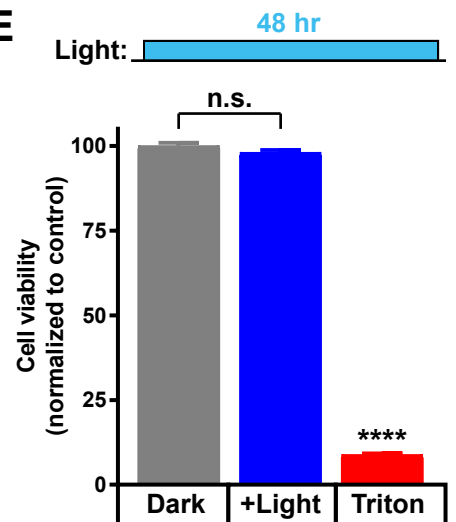


Figure S7. ReNcell VM cortical differentiation yields a highly neuronally-enriched culture, Related to Figure 6.

(A) ReNcell VM neuronal differentiation protocol schematic. (B) Representative immunofluorescence images of ReNcell VM neurons (differentiation day 18) following the differentiation protocol outlined in (A). MAP2 (green) and β III-tubulin (red) are shown at 20X (top) and 60X (bottom) magnification. (C) Quantification of the percentage of MAP2/ β III-tubulin double-labeled cells shows a highly enriched neuronal population following the outlined differentiation protocol. $n = 260$ cells. (D-E) ReNcell neurons were exposed to chronic blue light stimulation (48 hr, ~ 0.3 mW/cm², 465 nm) or darkness prior to examination of neuronal morphology (D) and cell viability, as assessed by measurements of ATP levels (E) (CellTiter-Glo, Promega). No differences in morphology (D) or cell viability (E) were observed between neurons in blue light or darkness conditions. Treatment with 0.1% Triton X-100 served as a positive death control. Scale bars = 20 μ m.

Supplementary Table 1. ALS/FTD patient information and scoring, related to Figures 3 and 4

Supplementary Table 2. Primer Sequences and cloning information, related to Star Methods

Movie S1. optoTDP43 chronic stimulation longitudinal imaging, related to Figure 1

Movie S2. optoTDP43 inclusion FRAP analysis, related to Figure 1

Movie S3. Cry2PHR vs optoLCD light induced phase separation, related to Figure 2

Movie S4. optoLCD vs. optoLCD^{M377V}, optoLCD^{Q331K}, and optoLCD^{A321V} repetitive light induced phase separation, related to Figure 2

Movie S5. Lack of optoTDP43 light induced phase separation, related to Figure 3

Movie S6. Cry2olig LCD RRM and FUS RRM + LCD light induced phase separation, related to Figure 4

Movie S7. Cytoplasmic TDP-43 FRAP within and outside of G3BP+ stress granules, related to Figure 5

Movie S8. optoTDP43 neuronal survival imaging, related to Figure 6

Movie S9. Cry2-mCh neuronal survival imaging, related to Figure 6